Indian Journal of Pure & Applied Physics
Vol. 48, February 2010, pp. 104-109

Characterisation and magnetic properties of nanocrystalline $FePO_4$

Marykutty Thomas[1*] & K C George[2]

[1]Department of Physics, B C M College, Kottayam 686 001, Kerala

[2]Department of Physics, S B College, Changanacherry 686 101, Kerala

*E-mail: marykutythomas@yahoo.co.in

Received 26 August 2009; revised 27 October 2009; accepted 30 November 2009

Nanocrystalline $FePO_4$ prepared by chemical method has been characterized using TG/DTA, XRD, TEM and FTIR. Magnetic studies have been carried out using VSM, SQUID magnetometry and ESR measurements. The $FePO_4$ for three reactant concentrations ($1ML^{-1}$, $0.1ML^{-1}$, $0.02M\ L^{-1}$) has been prepared and the effect of reactant concentration on particle size and hence, on magnetic properties is studied. Magnetic susceptibility and ESR measurements support each other and $FePO_4$ is found to be an anisotropic antiferromagnet with a Neel temperature of 21 K. As particle size decreases, the magnetic moment at room temperature decreases indicating magnetic moment disorder on the surface of smaller particles.

Keywords: Nanocrystalline $FePO_4$, Reactant concentration, IR spectrum, ESR, Magnetic susceptibility, Neel temperature

1 Introduction

Nanocrystalline and ultrafine particles of material are of great interest since they differ considerably from their bulk counterparts[1-3]. These materials are technologically important because surface to volume ratio of atoms is large compared to their bulk counterparts[4]. Nanosized oxide powders are used as ceramic material in industry[5] and magnetic material[4]. Iron phosphate [$FePO_4$] is one such material having catalytic activity in various industrially important reactions[6-9]. It is an important inorganic and biomaterial[10] possessing, a phenomenon known as structural memory[11]. Applied pressures of 2-3 GPa can transform this crystalline material to amorphous, coexisting with another crystalline phase. When the pressure is reduced, it can regain the original structure[12].

At room temperature, iron phosphate (ferric phosphate) has the berlinite [$AlPO_4$] structure which is closely related to that of α-quartz having iron and phosphorus tetrahedrally co-ordinated with oxygen[13-15]. $FePO_4$ has been studied as a ferroelectric material[15,16]. It is antiferromagnetically ordered below 25 K[11,13] and as a whole is a less studied magnetic material. In the present study, nanophase ferric phosphate is prepared and characterized by different techniques. The magnetic properties of this material may differ substantially from their bulk counterparts due to the large number of surface magnetic ions having lower co-ordination and broken exchange bonds[17].

The preparation methods needed to obtain well defined chemical microstructure depend on the conditions of synthesis. In this study nanocrystalline $FePO_4$ has been prepared by the thermolysis of polymer matrix based precursor solution constituted of aqueous solutions of iron nitrate, ammonium dihydrogen phosphate and sucrose which act as the fuel in the process[5]. The sample for three reactant concentrations has been prepared in order to study how the reactant concentration affects the particle size and hence magnetic properties. The crystalline powder obtained after heat treatment of the precursor powder was characterized by TEM, XRD and IR techniques and the magnetic properties were studied using VSM, SQUID magnetometry and ESR measurements. Since bulk $FePO_4$ is a paramagnetic material which is antiferromagnetically ordered at 24 K, it is interesting to investigate how the particle size or crystalline size affect the magnetic property of this material.

2 Experimental Details

Nanocrystalline $FePO_4$ was synthesised by chemical method[5]. The sample is prepared for three reactant concentrations, ie.,$1ML^{-1}$, $0.1ML^{-1}$ and $0.02\ ML^{-1}$, respectively. The stoichiometric amounts of iron nitrate, ammonium dihydrogen phosphate, aqueous solution of PVA (the matrix) and the aqueous solution of sucrose (the fuel) are mixed together and evaporated to a viscous liquid with the evolution of brown fumes of the decomposed nitrates. Here the cations are atomistically distributed throughout the

polymer structure, so that selective precipitation is prevented during the evaporation process. The fluffy voluminous carbonaceous mass produced during the complete evaporation of the precursor solution is thermolysed in the furnace at a maximum temperature of 650°C to get the nanocrystalline pinkish white $FePO_4$ powder. The precursor powder, black in color (carbonaceous dry mass) is subjected to TG/DTA analysis in argon (inert) atmosphere at a heating rate of 10°C/ min.

The fine powder of $FePO_4$ is used for the study of XRD, FTIR and TEM imaging. XRD profiles were taken by Philips (1710 PW) powder X-ray diffractometer using Cu Kα radiation over a wide range of Bragg angle. The FTIR spectrum was taken by Nicolet Avatar 360-ESP spectrometer. TEM imaging was carried out in a Philips CM-200-Analytical Transmission Electron Microscope working at 120 kV. Room temperature magnetic measurements were carried out by EG and G model 155 vibrating sample magnetometer (VSM). The ESR investigations were carried out using a standard reflection type X-band (9.25 GHz) spectrometer equipped with a Varian microwave cavity and a variable temperature cryostat system. Measurements of magnetisation as a function of temperature were done on a commercial superconducting quantum interference device (SQUID) magnetometer.

3 Results and Discussion

Figure 1 shows the TG/DTA curves of the precursor powder. A weight loss of 45% was noted in the TG curve over the temperature region 50-650°C. There are three endothermic peaks in the DTA curve. The peak at 125°C is due to dehydration and the peak at 560°C is due to decomposition of the precursor powder forming crystalline pinkish white ferric phosphate (α-$FePO_4$). The small endothermic peak at 712° is due to structural transformation, i.e. α to β transition without any mass loss[7]. The TG curve shows weight loss up to 650°C and there after there is no considerable weight loss.

Figure 2 shows the XRD pattern of $FePO_4$ for three reactant concentrations (1 ML^{-1}, 0.1 ML^{-1} and 0.02 ML^{-1}). The patterns suggest the formation of single phase crystalline compounds (JCPDS, card No. 29-715). The patterns appear to be the same for all molarities (reactant concentrations) and the crystallite size calculated using Scherrer formula is found to be in between 40-50 nm. There is only slight variation in crystalline size with molarity. The TEM image of 0.1 ML^{-1} $FePO_4$ (Fig. 3) shows that the particle size varies from 70-80 nm and are almost spherical but agglomerated. It is reported that for some ferric phosphate, the particles may fuse under an intense electron beam in Transmission Electron Microscope[18]. That may be a reason for the agglomeration of the particles observed in TEM image.

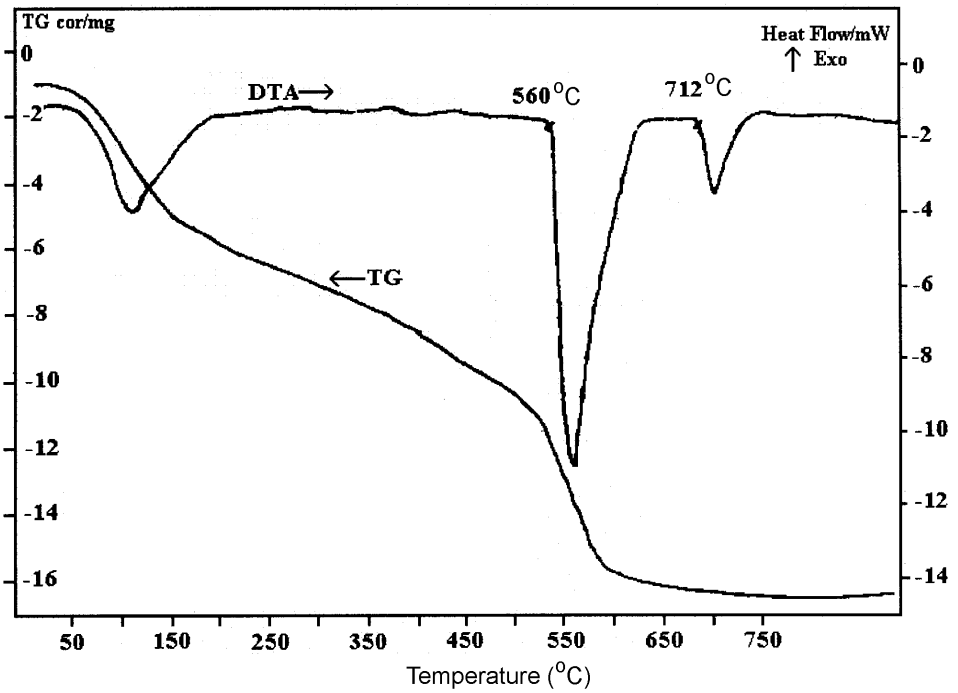

Fig. 1 — TGA/DTA curves of precursor powder

Figure 4 shows the FTIR spectrum of nano $FePO_4$ for three reactant concentrations. The probable band assignments for bulk $FePO_4$ are stretching vibrations of P-O (PO_4) around 1030 cm^{-1}, Fe-O vibrations around 630 cm^{-1} and O-P-O bending around 420 cm^{-1} excluding O-H (H_2O) vibrations[6,7,10,18]. Figure 4 shows a broad band (1000-1200 cm^{-1}) indicating the coupling of basic structural units (PO_4) into a structural network and it is reported that the coupling is very strong for $FePO_4$ (α-quartz like structure)[6]. It can be observed from this figure that the broadening is maximum for 0.02 ML^{-1} sample. It can also be noted that a change in frequency (blue shift) is observed for the basic (PO_4) structural vibration when the molarity changes from $1ML^{-1}$ to

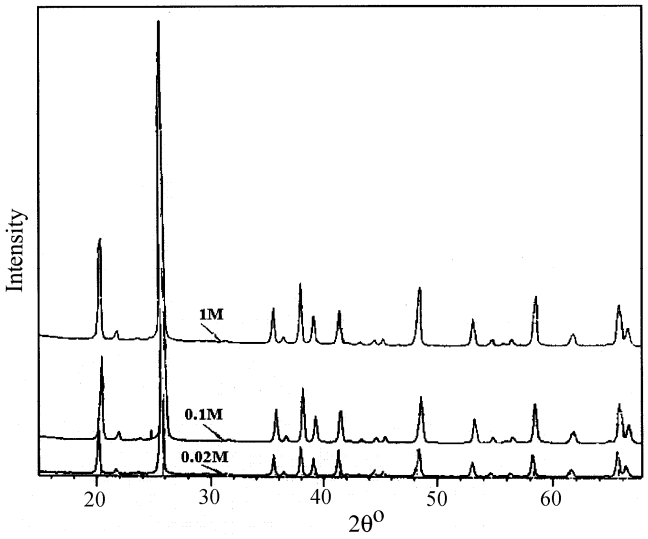

Fig. 2 — XRD pattern of $FePO_4$ for three reactant concentrations

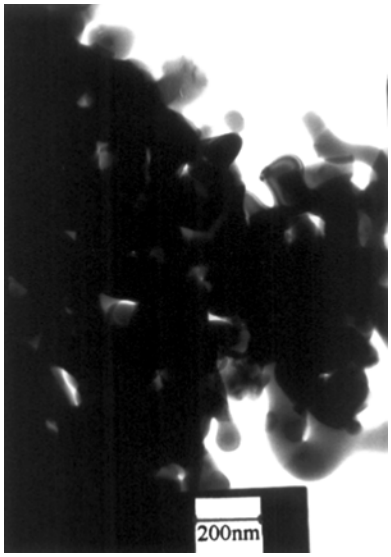

Fig. 3 — TEM image of $0.1ML^{-1}$ $FePO_4$ sample

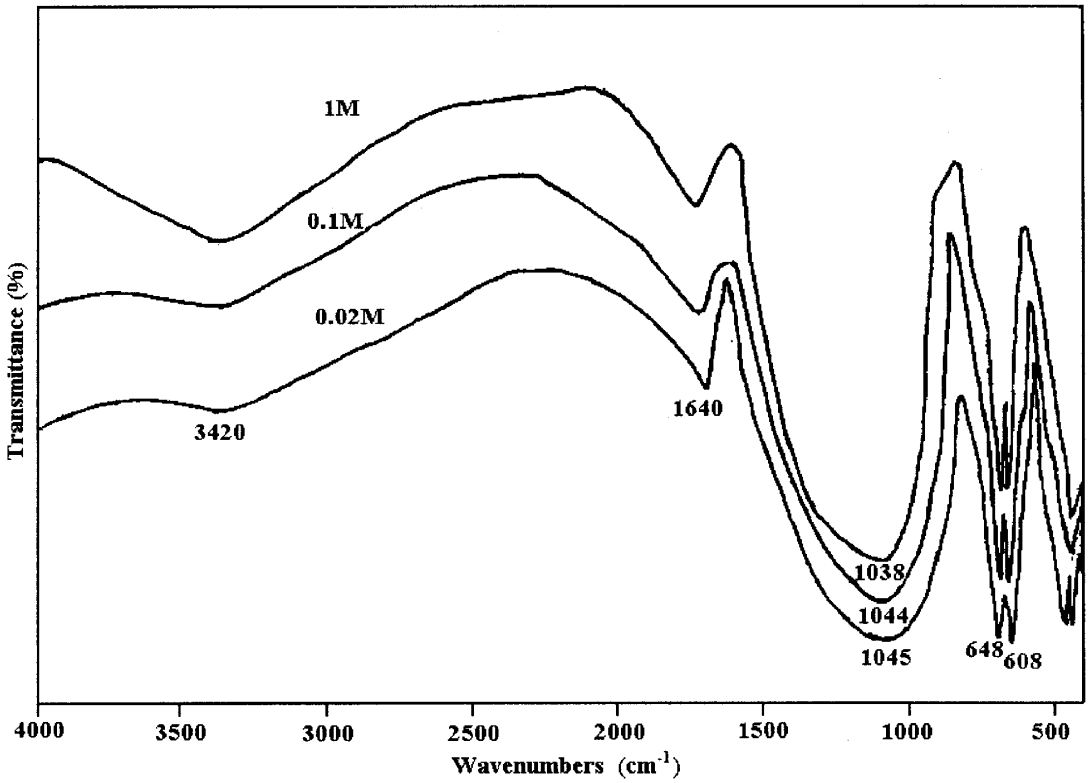

Fig. 4 — FTIR spectrum of $FePO_4$ for three reactant concentrations

0.02 ML^{-1}. Blue shift was observed in the case of nano Ag_3PO_4 with decrease in molarity[19]. For nanoparticles, small changes in the environment of the chemical group (PO_4) will lead to small changes in the characteristic vibrational frequencies for that group[20]. In addition the bond length will decrease with decrease in particle size. Hence an increase in band frequency (blue shift) may have resulted in the case of nano $FePO_4$ particles, indicating smallest particle size for 0.02 ML^{-1} sample. There are two nearby bands at 608 and 648cm^{-1} which are specific for $FePO_4$ structure and correspond to Fe-O vibrations[6]. These bands remain the same for all molarities. The bands below 500 cm^{-1} are assigned to O-P-O bending vibrations.

Figure 5 shows the variation of magnetic moment (emu/gm) with external magnetic field (k Gauss) for three reactant concentrations (1 ML^{-1}, 0.1 ML^{-1}, 0.02 ML^{-1}). These readings were recorded with VSM at room temperature. The molar susceptibility ψ_m was calculated and Fig. 6 shows the variation of molar susceptibility (Bohrmagneton) with reactant concentration (ML^{-1}). As the particle size decreases, the disorder of the magnetic moment orientation increases resulting in decrease of magnetic moment[21,22]. It is found that magnetic moment and molar susceptibility varies with reactant concentration and is minimum for 0.02ML^{-1} sample having smallest particle size.

Figure 7 shows the temperature variation of zero field cooling (ZFC) and field cooling (FC) magnetic susceptibilities of 0.02 ML^{-1} sample. Here the ZFC and FC susceptibilities coincide at high temperature, while at lower temperature they start to separate reaching a maximum value of ψ corresponding to 26°C. In antiferromagnetic material, the peak in ψ occurs at a temperature called Neel temperature (T_N). It is reported that the actual value of Neel temperature is few percent lower than the peak value[23-25]. In present

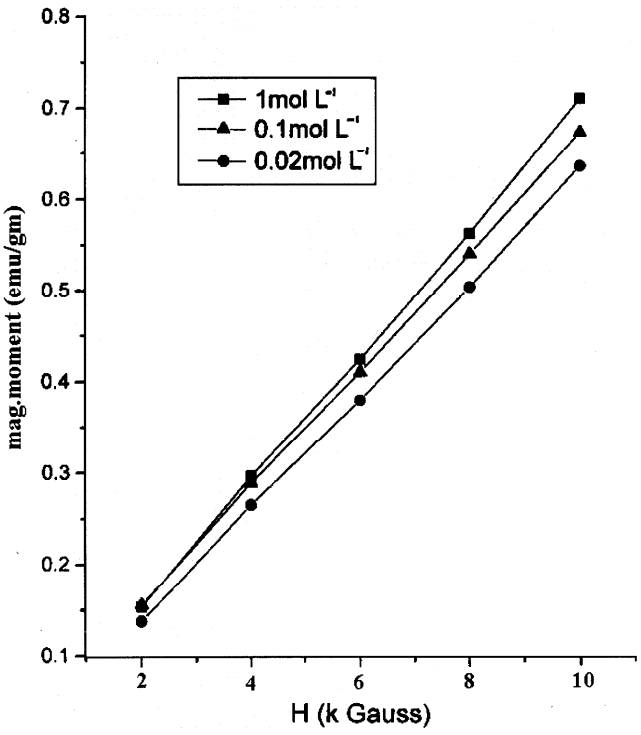

Fig. 5 — Variation of magnetic moment with external magnetic field at room temperature

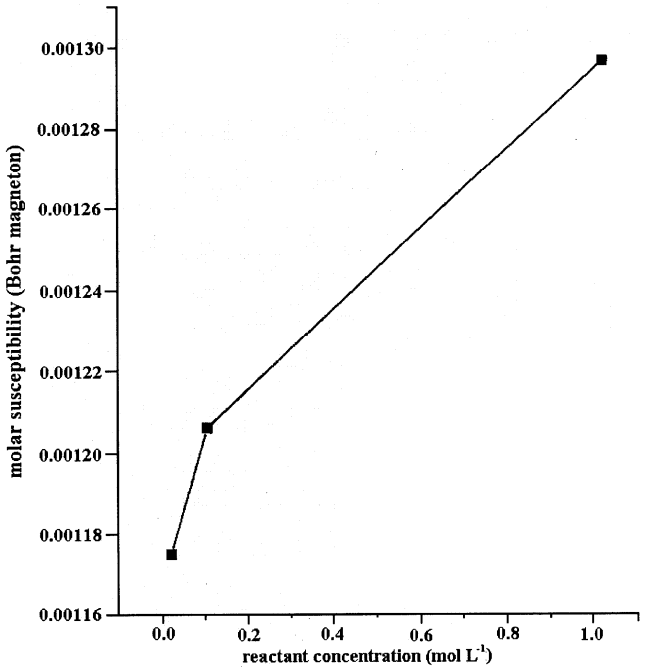

Fig. 6 — Variation of molar susceptibility with reactant concentration

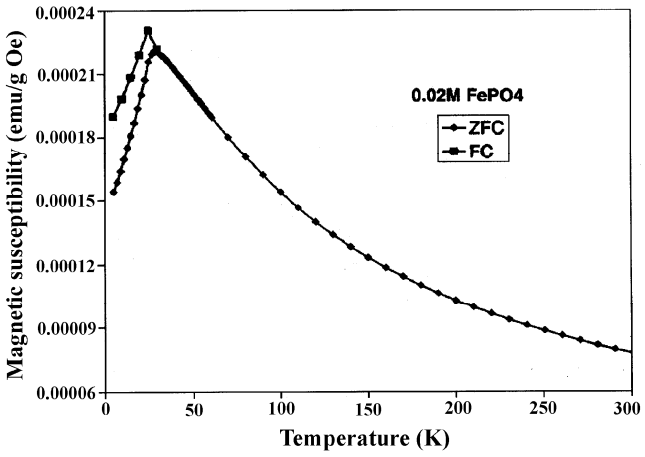

Fig. 7 — Temperature variation of ZFC and FC magnetic susceptibilities of 0.02 ML^{-1} sample

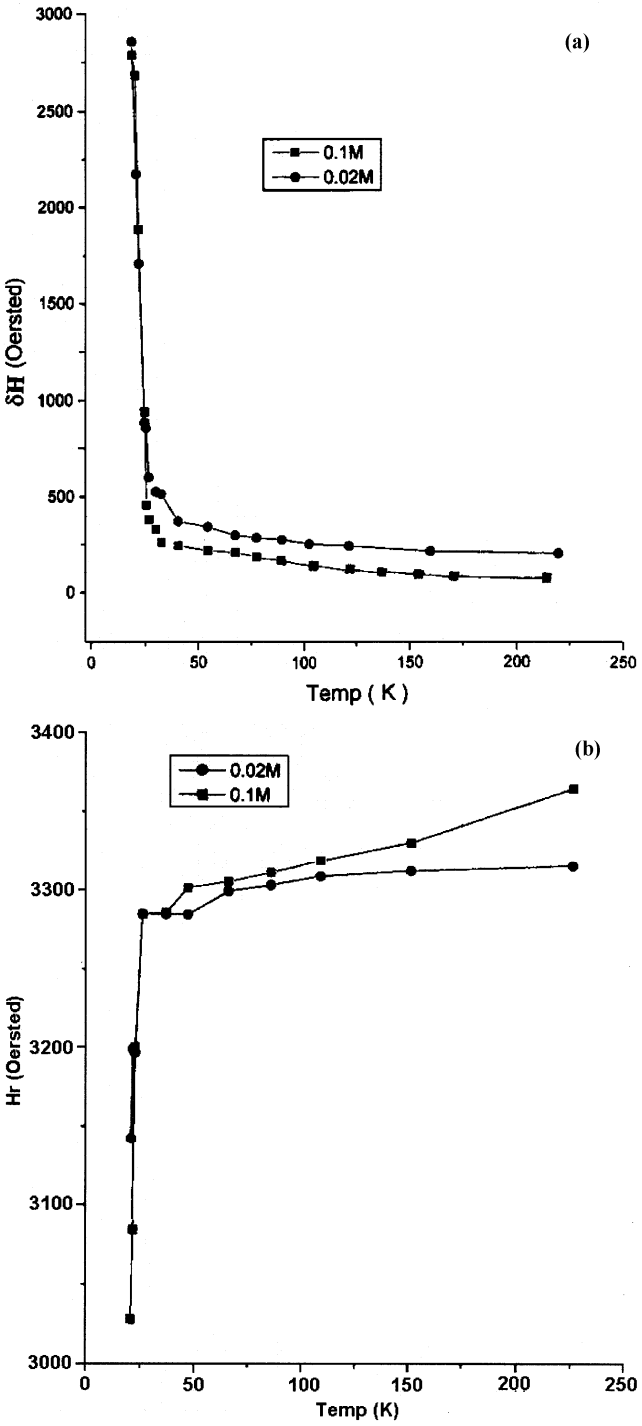

Fig. 8 — Temperature variation of (a) ESR line width, (b) resonance field of ESR spectrum

case the peak value is 26°C and the actual value of Neel temperature will be less than this value. The ψ–T data above T_N fits well with the Curie-Weiss law, $\psi = C/T - \theta$.

Figures 8a and 8b show the temperature variation of ESR line width (δH) and resonance field (Hr). The

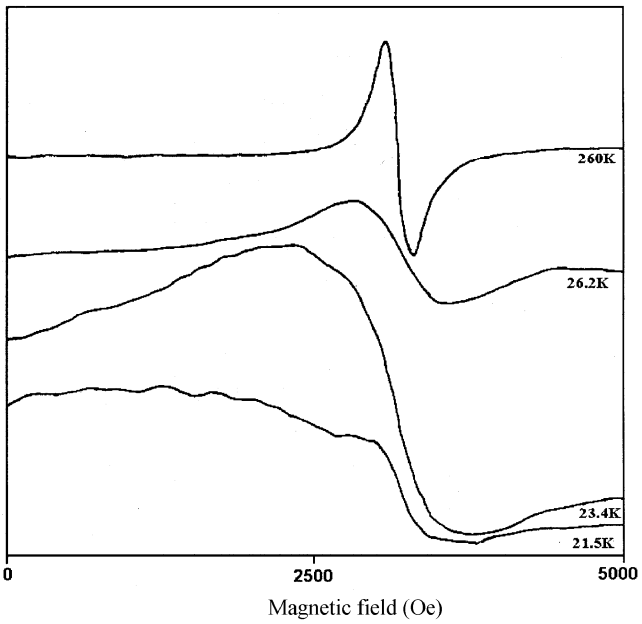

Fig. 9 — Temperature dependence of ESR spectrum

line width reported here is the peak to peak separation in the absorption derivative. Large increase in the line width (δH) and shifts of the resonance field (Hr) to lower fields can be observed as the temperature decreases. It is known that the ESR line broadens out on approach to T_N from high temperature side and it is the characteristic of anisotropic antiferromagnet[23,26]. It is observed that the Neel temperature, which is characteristic of antiferromagnetic ordering is 21 K for 0.1 ML^{-1} sample and 20.8K for 0.02 ML^{-1} sample. From this it can be inferred that T_N decreases with decrease in molarity (decrease in particle size). It can also be confirmed that the peak in ψ–T graph (26 K) is few degree higher than the actual T_N value (21 K) obtained from ESR studies.

Figure 9 shows the temperature dependence of derivative of ESR spectrum of 0.02 ML^{-1} sample. At low temperature, the line shape is asymmetric and at high temperature, symmetric line shape is obtained. At low temperature the anisotropy energy barrier is larger than the thermal fluctuations and the absorption will be distributed along the random direction of the anisotropy axes, providing an asymmetric line shape. The effect of temperature will be that of providing a progressively sharper and less asymmetrical line. At higher temperatures, when the relaxation of the magnetization through the anisotropy energy barrier is much faster, the thermal fluctuations will smear out the influence of anisotropy. The resonance spectrum is just like a normal paramagnetic resonance spectrum[27].

4 Conclusions

Nanocrystalline $FePO_4$ particles have been prepared by chemical method. The particle size variation with reactant concentration using XRD pattern is found to be small. But there is considerable change in IR spectroscopic frequency with reactant concentration indicating that particle size decreases with reactant concentration. It is found that nanophase $FePO_4$ is an antiferromagnet with axial anisotropy. The Neel temperature changes from 21 to 20.8K when the reactant concentration changes from 0.1 to $0.02ML^{-1}$. The magnetic moment measured at room temperature decreases with decrease in particle size.

References

1 Gleiter H, *Acta Materialia,* 48 (2000) 1.
2 Suryanarayana C, *Bull Mater Sci,* 17 (1994) 307.
3 Louis Bros, *J Phys Chem Solids*, 59 (1998) 459.
4 Punnoose A, Magnone H & Seehra M S, *Phys Rev B*, 64 (2001) 174420.
5 Pramanik P, *Bull Mater Sci*, 22 (1999) 335.
6 Prokupkova P, Koudelka L& Mosner P, *J Mater Sci*, 31 (1996) 3391.
7 Silvera Scaccia, Maria Carewska, Angelo Di Bartolomeo & Pier Paolo Prosini, *Thermochim Acta*, 383 (2002) 145.
8 Ai M & Ohdan K, *Appl Catal A*, 180 (1999) 47.
9 Dinamani M & Vishnu Kamath P, *Mater Res Bull*, 36 (2001) 2043.
10 Pierri E, Tsamouras D & Dalas E, *J Crystal Growth*, 213 (2000) 93.
11 Pasternak M P, Rozenberg G Kh, Milner A P*, et al*., *Phys Rev Lett,* 79 (1997) 4409.
12 Pasternak M P, Rozenberg G Kh, Milner A P, *et al*., *J Magn Magn Mater,* 183 (1998) 185.
13 Battle P D, Cheetham A K, Gleitzer C, *et al*., J *Phys C: Solid State Phys,* 15 (1982) L 919.
14 Ng H N & Calvo C, *Can J Chem,* 53 (1975) 2064.
15 Aliouane N, Badeche T, Gagou Y, Nigrelli E & Saint–Gregoire P, *Ferroelectrics,* 241 (2000) 255.
16 Philippot E, Goiffon A, Ibanez A & Pintard M, *J Solid State Chem,* 110 (1994) 356.
17 Seehra M S, Punnoose A, Roy P & Manivannan A, *IEEE Trans Magn,* 37 (2001) 2207.
18 Richard B Wilhelmy & Egon Matijevic, *Colloids and Surfaces,* 22 (1987) 111.
19 Marykutty Thomas, Ghosh S K & George K C, *Mater Lett,* 56 (2002) 386.
20 Harisingh Nalwa(Ed), *Handbook of Nanostructured materials and nanotechnolog* , Vol. 2 (Academic Press, New York), 2000.
21 Hochepied J F, Bonville P & Pileni M P, *J Phys Chem B*, 104 (2000) 905.
22 Gang Xiong & Zhen Hong Mai, *J Appl Phys*, 88 (2000) 519.
23 Punnoose A, Magnone H & Seehra M S, *IEEE Trans Magn*, 37 (2001) 2150.
24 Fisher M E, *Philos Mag*, 7 (1962) 1856.
25 Bragg E E & Seehra M S, *Phys Rev B*, 7 (1973) 4197.
26 Blinc R, Ceve P & Arcon D, *Phys Rev B,* 63 (2001) 212401.
27 Cannas C, Gatteschi D, Musinu A, Piccaluga G & Sangregorio C, *J Phys Chem B*, 102 (1998) 7721.